Use of a Soluble Epoxide Hydrolase Inhibitor in Smoke-Induced Chronic Obstructive Pulmonary Disease

Lei Wang[1], Jun Yang[2], Lei Guo[1], Dale Uyeminami[1], Hua Dong[2], Bruce D. Hammock[2], and Kent E. Pinkerton[1]

[1]Center for Health and the Environment, and [2]Department of Entomology and Cancer Center, University of California at Davis Medical Center, University of California at Davis, Davis, California

Tobacco smoke-induced chronic obstructive pulmonary disease (COPD) is a prolonged inflammatory condition of the lungs characterized by progressive and largely irreversible airflow limitation attributable to a number of pathologic mechanisms, including bronchitis, bronchiolitis, emphysema, mucus plugging, pulmonary hypertension, and small-airway obstruction. Soluble epoxide hydrolase inhibitors (sEHIs) demonstrated anti-inflammatory properties in a rat model after acute exposure to tobacco smoke. We compared the efficacy of sEHI t-TUCB (*trans*-4-{4-[3-(4-trifluoromethoxy-phenyl)-ureido]-cyclohexyloxy}-benzoic acid) and the phosphodiesterase-4 (PDE4) inhibitor Rolipram (Biomol International, Enzo Life Sciences, Farmingdale, NY) to reduce lung injury and inflammation after subacute exposure to tobacco smoke over a period of 4 weeks. Pulmonary physiology, bronchoalveolar lavage, cytokine production, and histopathology were analyzed to determine the efficacy of sEHI and Rolipram to ameliorate tobacco smoke–induced inflammation and injury in the spontaneously hypertensive rat. Both t-TUCB and Rolipram inhibited neutrophil elevation in bronchoalveolar lavage. sEHI t-TUCB suppressed IFN-γ, while improving lung function by reducing tobacco smoke–induced total respiratory resistance and tissue damping (small-airway and peripheral tissue resistance). Increases in tobacco smoke–induced alveolar airspace size were attenuated by t-TUCB. Rolipram inhibited the production of airway mucus. Both t-TUCB and Rolipram inhibited vascular remodeling–related growth factor. These findings suggest that sEHI t-TUCB has therapeutic potential for treating COPD by improving lung function and attenuating the lung inflammation and emphysematous changes caused by tobacco smoke. To the best of our knowledge, this is the first report to demonstrate that sEHI exerts significant protective effects after repeated, subacute tobacco smoke–induced lung injury in a rat model of COPD.

Keywords: experimental animal models; anti-inflammatory agents; airway obstruction

Chronic obstructive pulmonary disease (COPD) is a major cause of morbidity and mortality worldwide, and is expected to become the third leading cause of death by 2020 (1). COPD is characterized by chronic airflow limitation, with progressive deterioration over time and limited reversibility after bronchodilator therapy (2). The pathology of COPD is complex and heterogeneous, demonstrating inflammation, small-airway remodeling, the hypersecretion of mucus, and emphysema. The primary cause of COPD is tobacco smoke, which induces leukocyte activation, cytokine production, enhanced proinflammatory gene expression, increased reactive oxygen and nitrogen species production, and enhanced biosynthesis of oxidized lipids (3–6).

According to a commonly held belief, anti-inflammatory therapy for COPD may slow disease progression. Current COPD therapy mainly focuses on reducing symptoms and preventing exacerbation with short-acting and long-acting bronchodilators as monotherapy, or in combination with long-acting β_2 agonist bronchodilators and inhaled corticosteroids (7). The failure of inhaled corticosteroid used alone or in combination with β_2 agonists to reduce COPD inflammation has intensified the search for effective drugs for the disease (2, 8). Because COPD is relatively insensitive to currently marketed drugs (9), it is hoped that novel, anti-inflammatory agents will be found.

Phosphodiesterase-4 (PDE4) inhibitors are the most advanced anti-inflammatory therapies currently used for the clinical management of COPD. The elevation of cellular cyclic adenosine monophosphate can lead to broad anti-inflammatory cellular effects, and PDE4 is the predominant PDE isoenzyme in most inflammatory cells thought to play a role in the pathogenesis of COPD (2). Despite reports of PDE4 inhibitor efficacy in Phase III clinical trials and the recent approval of Roflumilast by the European Medicines Agency for the treatment of COPD (10), the class-specific side effects (e.g., nausea and diarrhea) of the high-dose administration of these drugs limit their therapeutic use (11, 12).

Epoxyeicosatrienoic acids (EETs), products of the epoxygenation of arachidonic acid by cytochrome P450 monoxygenases,

CLINICAL RELEVANCE

Inflammation is provoked by inflammatory leukocytes and mediators thought to play a critical role in the development of chronic obstructive pulmonary disease (COPD). Soluble epoxide hydrolase inhibitors were shown to possess therapeutic efficacy in the treatment and management of acute inflammatory disease. It is not known whether soluble epoxide hydrolase inhibitors could ameliorate the pulmonary inflammation induced by repeated, subacute exposure to tobacco smoke. The efficacy of a potent soluble epoxide hydrolase inhibitor, *trans*-4-{4-[3-(4-trifluoromethoxy-phenyl)-ureido]-cyclohexyloxy}-benzoic acid, to partly ameliorate the impact of injury attributable to repeated exposure to tobacco smoke suggests that the inhibition of soluble epoxide hydrolase could have high therapeutic potential for the treatment of COPD.

(*Received in original form October 11, 2011 and in final form December 12, 2011*)

This work was supported by Tobacco-Related Disease Research Program grant 18XT-0154 and American Asthma Foundation grant 09-0269. B.D.H. is a George and Judy Marce Senior Fellow of the American Asthma Foundation. J.Y. was supported by an Elizabeth Nash Memorial Fellowship from Cystic Fibrosis Research, Inc.

L.W., J.Y., H.D., B.D.H., and K.E.P. designed and planned the research. L.W., J.Y., L.G., and D.U. performed the study, data collection, and statistical analysis. L.W. drafted the manuscript. J.Y., B.D.H., and K.E.P. provided editing and critical revisions during the preparation of the manuscript.

Correspondence and requests for reprints should be addressed to Kent E. Pinkerton, Ph.D., Center for Health and the Environment, University of California at Davis, Old Davis Road, Davis, CA 95616. E-mail: kepinkerton@ucdavis.edu

This article has an online supplement, which is accessible from this issue's table of contents at www.atsjournals.org

Am J Respir Cell Mol Biol Vol 46, Iss. 5, pp 614–622, May 2012

Originally Published in Press as DOI: 10.1165/rcmb.2011-0359OC on December 22, 2011
Internet address: www.atsjournals.org

exert antiinflammatory effects (13). EETs are metabolized by cyclooxygenase (COX) and the β-oxidation pathway, but most EETs are converted to diols by soluble epoxide hydrolase (sEH) (14). The pharmacological inhibition of sEH increases plasma EET concentrations (15). A large number of studies reported the lowering of blood pressure in different models of systemic hypertension (16), the prevention of cardiac remodeling after aortic banding (17), and the suppression of inflammation elicited by bacterial LPS (18) with the inhibition of sEH. We previously demonstrated anti-inflammatory effects with the sEH inhibitor 12-(3-adamantane-1-yl-ureido)-dodecanoic acid n-butyl ester after acute exposure to tobacco smoke in spontaneously hypertensive (SH) rats (19). In the present study, we characterize: (*1*) a model of tobacco smoke–induced COPD in SH rats to demonstrate COPD-like lung inflammation, airway obstruction, the hypersecretion of mucus, and emphysematous changes; and (*2*) the efficacy of *trans*-4-{4-[3-(4-**t**rifluoromethoxy-phenyl)-ureido]-cyclohexyloxy}-benzoic acid (t-TUCB), a newer generation of sEH inhibitor (sEHI), compared with the prototypic PDE4 inhibitor Rolipram on the attenuation of tobacco smoke–induced lung injury in SH rats. We found that t-TUCB has therapeutic potential for treating COPD by reducing lung inflammation and weight loss, improving lung function, and attenuating the emphysematous changes caused by exposure to tobacco smoke.

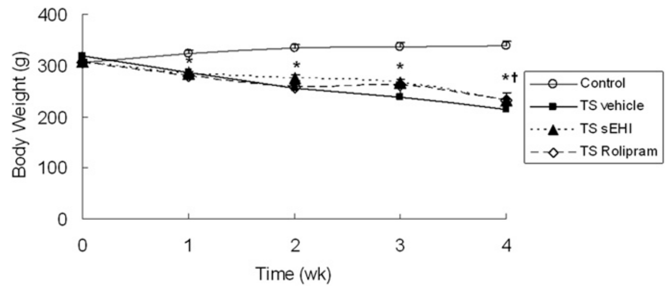

Figure 1. Effects of *trans*-4-{4-[3-(4-**t**rifluoromethoxy-phenyl)-ureido]-cyclohexyloxy}-benzoic acid (t-TUCB) and Rolipram on tobacco smoke (TS) exposure–induced weight loss in spontaneously hypertensive (SH) rats. Body weight measurements were taken before and after smoke exposure each week. The weekly mean weights measured before smoke exposure each week are reported. The time course is presented for body weight changes of age-matched, non–TS-exposed animals as controls (*open circles*), TS-exposed animals treated with vehicle (*solid squares*), TS-exposed animals treated with soluble epoxide hydrolase inhibitors (sEHI) t-TUCB (*solid triangles*), and TS-exposed animals treated with Rolipram (*open diamonds*). Data are expressed as means ± SEM for 4–8 animals/group. wk, weeks. *$P < 0.05$, TS-exposed groups were significantly different from the control group. †$P < 0.05$, treatment group with sEHI t-TUCB was significantly different from the TS vehicle group.

MATERIALS AND METHODS

Additional details on measurement methods are provided in the online supplement.

Animals

This study was performed under the auspices of the Animal Care and Use Committee of the University of California at Davis. Twelve-week-old male SH rats were purchased from Charles River Laboratories (Portage, MI) and allowed to acclimate 1 week before the onset of exposure to tobacco smoke.

Exposure to Tobacco Smoke

SH rats, divided into groups of 4 to 8 animals, were exposed to filtered air or tobacco smoke. Whole-body exposure to cigarette smoke occurred for 6 hours/day, 3 days/week for a total of 4 weeks at a concentration of 80 to 90 mg/m^3 total suspended particulates, using a TE10 smoke exposure system (20) that burns 3R4F research cigarettes (Tobacco and Health Research Institute, University of Kentucky, KY) with a 35-ml puff volume of 2-second duration, once each minute (smoking standard of the Federal Trade Commission).

Drugs and Delivery

We synthesized sEHI t-TUCB, whereas Rolipram was purchased from Biomol International (Enzo Life Sciences, Farmingdale, NY). Both compounds were delivered via drinking water 1 week before smoke exposure and continued throughout the 4-week study. We used doses of 1.5 mg/kg t-TUCB and 0.3 mg/kg Rolipram, dissolved in polyethylene glycol (PEG) 400 in drinking water, to give a final PEG concentration of 2% (vol/vol). Age-matched animals exposed only to filtered air with vehicle only in their drinking water served as sham controls.

Pulmonary Function Measurements

Eighteen hours after the end of tobacco smoke exposure, rats were deeply anesthetized with ketamine and xylazine. The trachea of each animal was cannulated and connected to a FlexiVent (Scireq, Montreal, PQ, Canada) data acquisition system. Animals were ventilated at a frequency of 90 breaths/minute, at a tidal volume of 10 ml/kg. Measures of respiratory system input impedance were obtained to allow for the unique distinction between central and peripheral lung mechanics. A "snapshot perturbation" maneuver was imposed to measure the resistance, compliance, and elastance of the whole respiratory system. Forced oscillation perturbation was consequently applied and resulted in central airway resistance, tissue damping, and tissue elastance.

Tissue Preparation

Immediately after pulmonary function testing, the trachea was recannulated, the left lung bronchus was tied, and the right lung was lavaged with Ca^{2+}/Mg^{2+}–free Hanks' buffered salt solution (HBSS). Bronchoalveolar lavage fluid (BALF) was collected in tubes and kept on ice until further processing. The lavaged lobes from the right lung were frozen in liquid nitrogen and stored at $-80^{\circ}C$ until use. The left lung was embedded in paraffin for histology.

Bronchoalveolar Lavage Analysis

BALF was centrifuged for 10 minutes at $4^{\circ}C$, and the cell pellet was resuspended in Ca^{2+}/Mg^{2+}–free HBSS (21). The total cell number was determined using a hemocytometer. BALF cell differentials were determined by counting the number of mononuclear cells, neutrophils, and eosinophils (300 cells/sample).

Cytokine Analysis of Lung Homogenates

Lung homogenates from rats were analyzed for 24 different cytokines and chemokines (IL-1α, IL-1β, IL-2, IL-4, IL-5, IL-6, IL-7, IL-10, IL-12p70, IL-13, IL-17, IL-18, eotaxin, granulocyte colony-stimulating factor, granulocyte/macrophage colony-stimulating factor, growth-related oncogene-KC/keratinocyte-derived chemokine, IFN-γ, macrophage colony-stimulating factor, macrophage inflammatory protein [MIP]-1α, MIP-3α, regulated upon activation, normal T cell expressed, and secreted, TNF-α, vascular endothelial growth factor [VEGF], and erythropoietin), using a fluorescent bead multiplex assay from Bio-Rad Laboratories (Hercules, CA). The assay was performed according to the manufacturer's instructions.

Oxylipin Measurements by Liquid Chromatography–Mass Spectrometry

Analysis of oxylipins from lung tissues was performed according to Yang and colleagues (22). Oxylipins were extracted by solid phase extraction. Elutions were evaporated and reconstituted with 50 μl

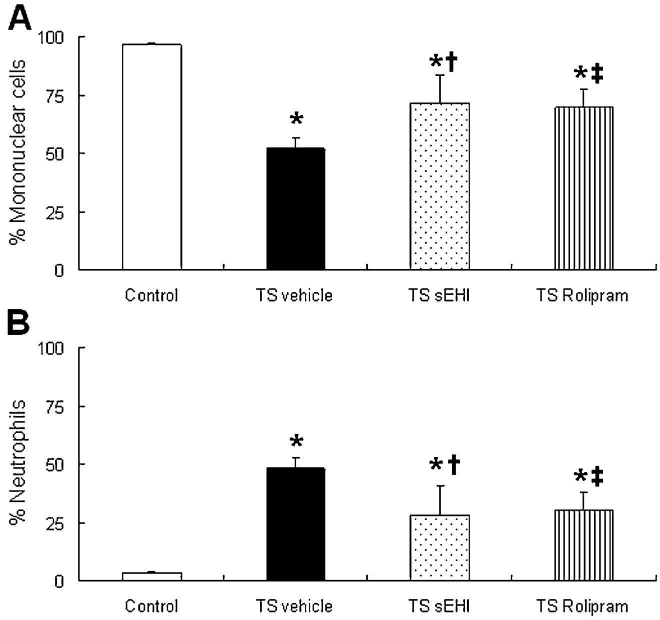

Figure 2. Effects of t-TUCB and Rolipram on leukocyte profile in bronchoalveolar lavage. (*A*) Percent of mononuclear cells (including macrophages, monocytes, and lymphocytes). (*B*) Percentages of neutrophils in the bronchoalveolar lavage (BAL). Data are expressed as means ± SEM for 4–8 animals/group. *$P < 0.05$, TS-exposed groups were significantly different from control group. †$P < 0.05$, treatment group with sEHI t-TUCB was significantly different from the TS vehicle group. ‡$P < 0.05$, treatment group with Rolipram was significantly different from the TS vehicle group.

200 nM 1-cyclohexyl ureido, 3-dodecanoic acid methanol solution. Liquid chromatography was performed on an Eclipse Plus C18 column (Agilent Corporation, Palo Alto, CA). Analytes were eluted according to their polarity, with the most polar analytes, prostaglandins, and leukotrienes eluting first, followed by hydroxy and epoxy fatty acids. Quality control samples were analyzed to ensure the stability of the analytical calibration throughout the analysis. Analyst software version 1.5 (AB Sciex, Foster City, CA) was used to quantify the results, according to standard curves.

Histopathologic Measurements of the Lung

Five-micrometer-thick sections of lung tissue were deparaffinized and stained with (*1*) hematoxylin and eosin (American Master Tech Scientific, Lodi, CA) for the measurement of alveolar airspace size, and (*2*) alcian blue/periodic acid–Schiff (AB/PAS; American Master Tech Scientific) for the detection of mucous glycoconjugate. To determine the fraction of epithelial mucosubstance staining, as well as the mean linear intercept (MLI) of alveoli, images were projected onto a monitor and overlaid with a test grid generated by Stereology Toolbox software (Morphometrix, Davis, CA). For details of the calculation for volume fractions and MLI, please see the online supplement.

Statistical Analysis

Data were analyzed using SAS version 8.2 statistical software (SAS Institute, Cary, NC). Two-way ANOVA was used, and when significance was achieved, a Bonferroni *post hoc* test was applied. For analysis of the correlation between oxylipins with airway obstruction based on FlexiVent measurements, linear regression was used to analyze correlations according to the Pearson correlation coefficient. $P < 0.05$ was considered significant.

RESULTS

Effects of sEHI t-TUCB and Rolipram on Body Weight after Exposure to Tobacco Smoke

Before exposure to tobacco smoke (TS), group body weights were similar. After 1 week of TS exposure, all three groups exposed to TS (TS vehicle, TS t-TUCB, and TS Rolipram) weighed significantly less than the control group exposed only to filtered air and vehicle (Figure 1). Weight loss continued through the 4-week exposure period for all three TS groups. However, the

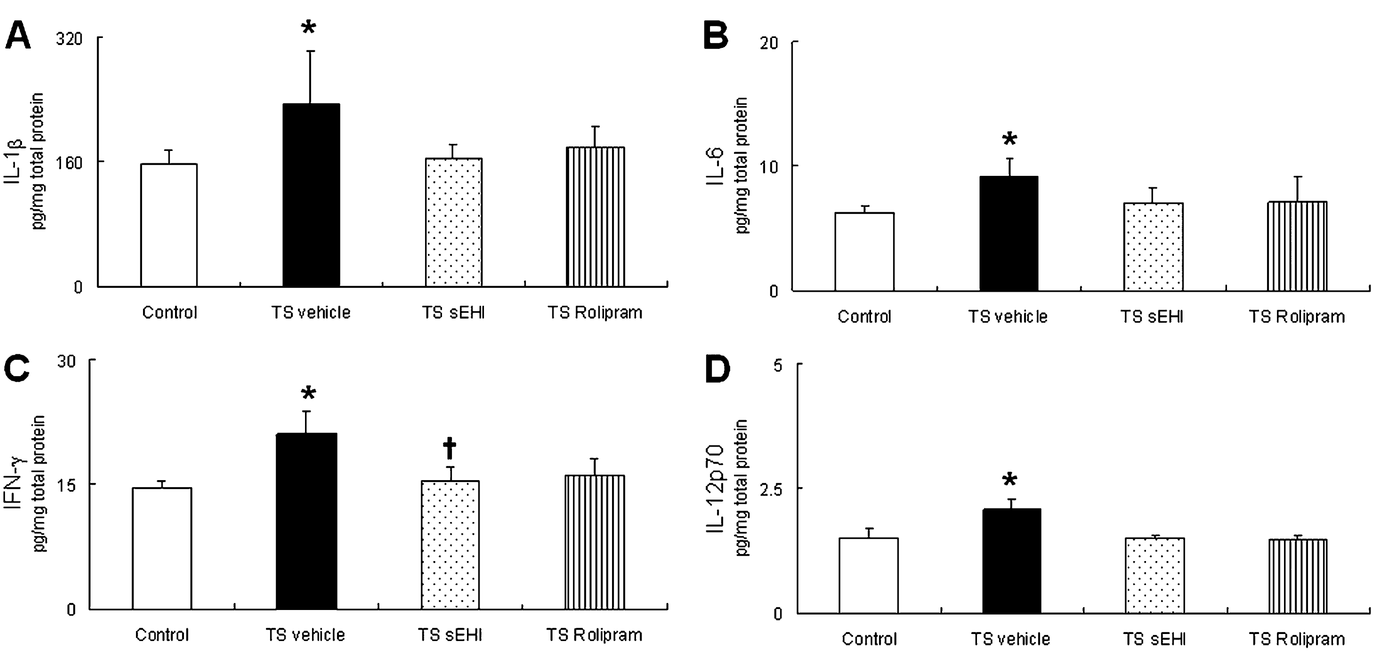

Figure 3. Effects of t-TUCB and Rolipram on pulmonary inflammatory cytokines. Inflammatory cytokine (*A*) IL-1β, (*B*) IL-6, (*C*) IFN-γ, and (*D*) IL-12p70 concentrations in whole-lung homogenate are reported. Data are expressed as mean ± SEM for 4–8 animals/group. *$P < 0.05$, TS-exposed groups were significantly different from the control group. †$P < 0.05$, treatment group with sEHI t-TUCB was significantly different from the TS vehicle group.

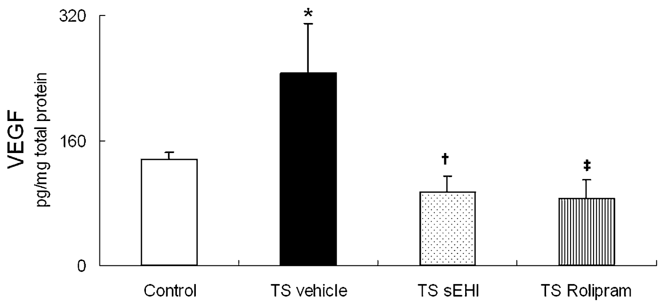

Figure 4. Effects of t-TUCB and Rolipram on vascular endothelial growth factor (VEGF) in the lung. Data are expressed as means ± SEM for 4–8 animals/group. *$P < 0.05$, TS-exposed groups were significantly different from the control group. †$P < 0.05$, treatment group with sEHI t-TUCB was significantly different from the TS vehicle group. ‡$P < 0.05$, treatment group with Rolipram was significantly different from the TS vehicle group.

degree of weight loss with TS t-TUCB treatment was significantly less compared with the TS vehicle group. Animals treated with Rolipram showed a trend similar to those treated with t-TUCB regarding weight loss, but the data did not achieve statistical significance.

Effects of t-TUCB and Rolipram on TS–Induced Leukocyte Recruitment to the Lung

In control rats, the majority of leukocytes recovered in the BALF were mononuclear cells (primarily macrophages), accounting for approximately 90% of the total cells (Figure 2A). Four weeks of repeated TS exposure resulted in significantly increased total leukocyte counts (89×10^3/ml versus 22×10^3/ml, $P < 0.01$) and neutrophil counts (67×10^3/ml versus 0.8×10^3/ml, $P < 0.001$) in the vehicle-only group compared with the filtered air plus vehicle control group, respectively. Whereas neutrophils consisted of 3.4% ± 0.6% of the total cells in the control BALF, they comprised 47.9% ± 4.4% in the BALF of the TS/vehicle group, a significant difference between the two treatment groups. TS exposure plus treatment with sEHI t-TUCB or the PDE4 inhibitor Rolipram markedly decreased the percentage of neutrophils in the BALF to 28% ± 12.7% and 30.2% ± 7.8%, respectively (Figure 2B). The dose of t-TUCB and Rolipram used in the present study did not significantly alter the increase in total leukocyte numbers in the BALF induced by TS exposure (data not shown).

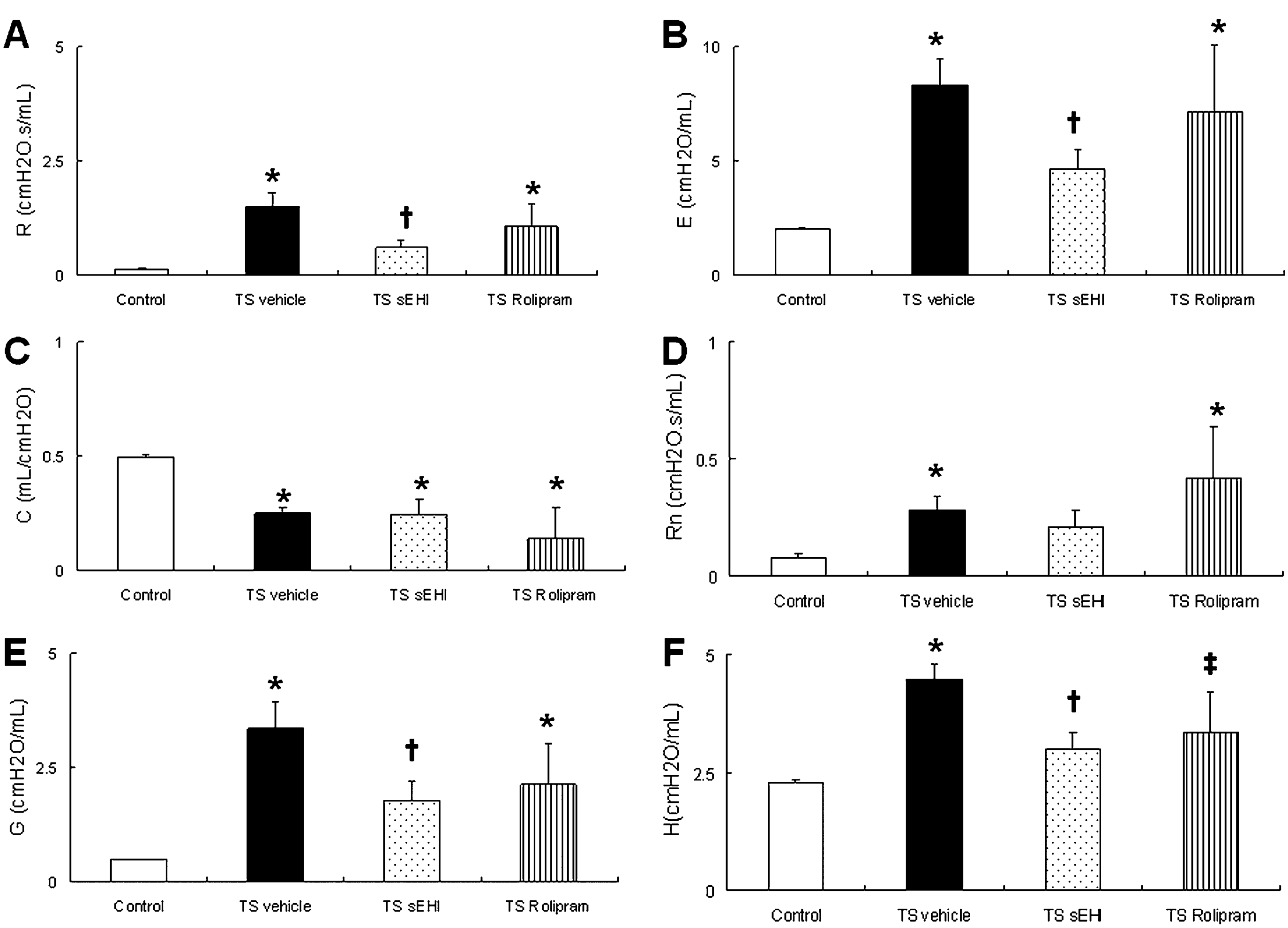

Figure 5. Effects of t-TUCB and Rolipram on pulmonary function in the lung. (*A*) Total respiratory resistance (R) and (*B*) elastance (E), (*C*) compliance (C), (*D*) central airway resistance (Rn), (*E*) tissue damping (G), and (*F*) elastance (H) are shown. Data are expressed as means ± SEM for 4–8 animals/group. *$P < 0.05$, TS–exposed groups were significantly different from the control group. †$P < 0.05$, treatment group with sEHI t-TUCB was significantly different from the TS vehicle group. ‡$P < 0.05$, treatment group with Rolipram was significantly different from the TS vehicle group.

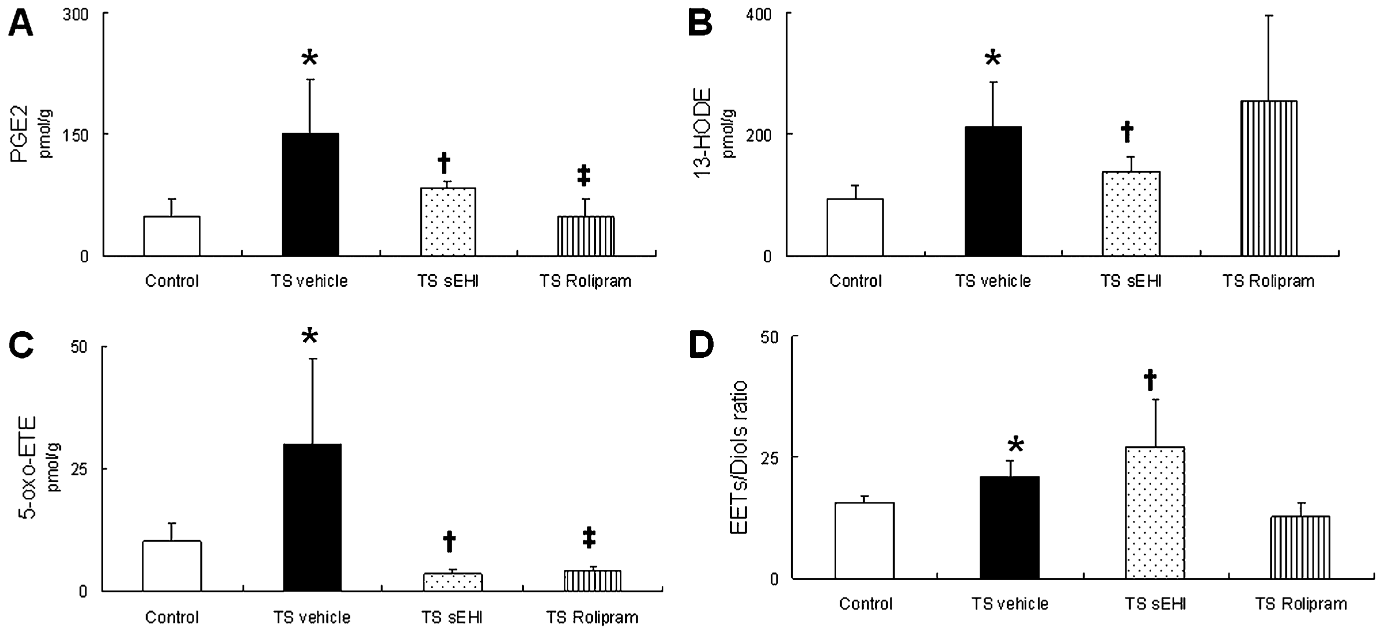

Figure 6. Effects of t-TUCB and Rolipram on oxylipins in the lung. (*A*) Major oxylipins prostaglandin E2 (PGE2), (*B*) 13-hydroxyoctadecadienoic acid, and (*C*) 5-oxo-6,8,11,14-eicosatetraenoic acid and (*D*) the epoxyeicosatrienoic acids (EETs)/diols ratio are shown. Data are expressed as means ± SEM for 4–8 animals/group. *$P < 0.05$, TS-exposed groups were significantly different from the control group. †$P < 0.05$, treatment group with sEHI t-TUCB was significantly different from the TS vehicle group. ‡$P < 0.05$, treatment group with Rolipram was significantly different from the TS vehicle group.

Effects of t-TUCB and Rolipram on Inflammatory Cytokines and VEGF in Lung Homogenate

The increase in neutrophils after 4 weeks of TS exposure in the vehicle-only group was accompanied by significant increases in proinflammatory cytokines IL-1β and IL-6 and Th1 cytokines IFN-γ and IL-12p70 in lung homogenate (Figures 3A–3D). Exposure to TS plus treatment with t-TUCB or Rolipram did not result in the significantly inhibited production of inflammatory cytokines IL-1β or IL-6, but tended to decrease Th1 cytokines, such as IFN-γ. In fact, the concentration of IFN-γ was significantly lower in animals treated with sEHI t-TUCB compared with the TS and vehicle groups. VEGF protein expression was significantly increased in rats exposed to TS and vehicle, compared with control rats. This results was in contrast to a significant decrease in VEGF compared with control rats exposed to TS and either t-TUCB or Rolipram (Figure 4).

Effects of t-TUCB and Rolipram on Pulmonary Function

Exposure to TS for 12 days over a 4-week period produced significant changes in lung function. TS-exposed and vehicle-treated animals had significantly elevated total respiratory resistance (R) and elastance (E) accompanied by significantly decreased compliance (C), compared with control rats. Central airway resistance (Rn), tissue damping (G), and elastance (H) were also significantly increased by TS and vehicle exposure. On the other hand, TS exposure plus treatment with sEHI t-TUCB significantly improved lung mechanics by decreasing R and E, as well as small airway and peripheral tissue resistance and elastance. Animals treated with Rolipram did not show significant improvement in lung function (Figures 5A–5F).

Effects of t-TUCB and Rolipram on Lung Oxylipins

Regulatory lipids were measured to monitor changes in active lipid mediators, including prostaglandins, leukotrienes, and EETs. To assess the degree of sEH inhibition, the ratio of EETs to their corresponding dihydroxy derivatives (diols) was calculated. Prostaglandin E2 (PGE2), 13-hydroxyoctadecadienoic acid (13-HODE), and 5-oxo-6,8,11,14-eicosatetraenoic acid (5-oxo-ETE) were significantly increased after 4 weeks of exposure to TS and vehicle (Figures 6A–6C). In addition, these animals had a significantly decreased EETs/diols ratio, implying an increase in either sEH protein expression or sEH activity (Figure 6D). The administration of sEHI t-TUCB, along with exposure to TS, significantly decreased proinflammatory mediator

TABLE 1. CORRELATION BETWEEN OXYLIPINS AND AIRWAY OBSTRUCTION IN SH RATS

Characteristic	R	Rn	G
PGE2	$r = 0.3$, $P = 0.1552$	$r = 315$, $P = 0.17$	$r = 0.212$, $P = 0.36$
13-HODE	$r = 0.436$, $P = 0.031$*	$r = 0.529$, $P = 0.01$*	$r = 0.355$, $P = 0.12$
5-oxo-ETE	$r = 0.032$, $P = 0.86$	$r = 0.077$, $P = 0.74$	$r = 0.292$, $P = 0.20$
EET/diols ratio	$r = 0.214$, $P = 0.31$	$r = 0.032$, $P = 0.92$	$r = 0.197$, $P = 0.39$

Definition of abbreviations: 5-oxo-ETE, 5-xox-6,8,11,14-eicosatetraenoic acid; 13-HODE, 13-hydroxyoctadecadienoic acid; EET, epoxyeicosatrienoic acid; G, tissue damping; PGE2, prostaglandin E2; *r*, Pearson's correlation coefficient; R, respiratory resistance; Rn, airway resistance; SH, spontaneously hypertensive.

* $P < 0.05$, significance level.

concentrations of PGE2, 13-HODE, and 5-oxo-ETE, compared with rats exposed to TS and vehicle. As expected, the EETs/diols ratio was significantly increased by t-TUCB treatment compared with that of animals exposed to TS and vehicle. Rats receiving Rolipram along with TS exposure had significantly decreased PGE2 and 5-oxo-ETE concentrations, compared with rats exposed to TS and vehicle. No difference in the EETs/diols ratio was evident in rats treated with Rolipram, compared with rats exposed to TS and vehicle (Figures 6A–6D). Strong, positive correlations were found between total respiratory resistance (R) and 13-HODE ($r = 0.436$, $P < 0.05$) and between central airway resistance (Rn) and 13-HODE ($r = 0.529$, $P < 0.01$) (Table 1).

Effects of t-TUCB and Rolipram on TS Exposure–Induced Mucosubstances and Airspace Enlargement

The excessive production of mucin is characteristic of advanced COPD. In this study, after 4 weeks of TS and vehicle exposure, animals demonstrated a significant elevation in the volume fraction of intraepithelial mucosubstances, as demonstrated by AB/PAS-positive staining compared with control animals. Treatment with t-TUCB alone did not change concentrations of airway epithelial mucin (Figure 7). However, animals receiving Rolipram had significantly decreased intraepithelial airway mucin compared with animals exposed to TS and vehicle only (Figure 7B).

Airspace enlargement, as quantified by the MLI, was significantly increased in all three groups exposed to TS,compared with the filtered air control group. Both sEHI t-TUCB and Rolipram treatment decreased MLI, but only treatment with t-TUCB reached a level of statistical significance to reduce MLI (Figure 8).

DISCUSSION

The exposure of SH rats to TS for 12 days over a period of 4 weeks produced classic pathophysiological features found in patients with COPD, including chronic pulmonary inflammation with significant elevations in neutrophil number, pulmonary cytokines, proinflammatory fatty acid diols, and PGE2, in addition to airway mucus hypersecretion, alveolar airspace enlargement, and weight loss, all consistent with previous findings in this model (23, 24). Marked airway obstruction was evidenced by significant increases in total respiratory resistance (R), central airway resistance (Rn) and peripheral tissue resistance (G). Given these findings, the SH rat TS model is highly plausible for testing the efficacy of compounds to treat COPD, even after as brief an exposure period to TS as 4 weeks. In the present study, both sEHI t-TUCB and the PDE4 inhibitor Rolipram exerted anti-inflammatory effects by reducing neutrophil influx in the BALF and reducing concentrations of proinflammatory oxylipins. Furthermore, sEH inhibition significantly improved lung function by decreasing airway resistance, while also lessening weight loss.

Airway obstruction is one of the key features of COPD. Using a small animal ventilator apparatus, we can accurately measure airway resistance and distinguish resistance between central airway and peripheral tissues. Airway resistance primarily reflects the specific degree of airway obstruction. In this study, we found a significant increase in airway resistance, which could have arisen from increased inflammation, mucus hypersecretion, and airway remodeling induced by repeated, subacute exposure to TS. Zheng and colleagues reported increased total respiratory resistance in a rat model of COPD induced by exposure to sidestream cigarette smoke for 36 weeks (25). Treatment with sEHI t-TUCB significantly improved lung function by decreasing airway resistance in both central airway and peripheral tissues, thus demonstrating that sHE inhibition improves lung function in a COPD animal model.

Inflammation in the lungs of patients with COPD affects both small and large airways, and is likely to be critical in the genesis and progression of the pathology of the disease. The degree of inflammation is associated with disease severity (6, 26). In this rat model of COPD, a 4-week TS exposure induced a robust inflammatory response that was strongly associated with the degree of airway obstruction. Both t-TUCB and Rolipram demonstrated anti-inflammatory effects, although they did not completely inhibit the inflammatory response induced by TS, as indicated by their lack of influence on the total number of leukocytes in BALF or whole-lung proinflammatory cytokines, IL-1β, and IL-6. sEHIs and selective PDE4 inhibitors were reported to inhibit total inflammatory cells in BALF induced by TS exposure or LPS challenge (3, 19, 27, 28). The disparity between our study and previous studies may be attributable to differences in dose or routes of drug administration. For example, Smith and colleagues (19) used a subcutaneous injection of sEHI at 10 mg/kg versus the 1.5 mg/kg used in the present study, and Kubo and colleagues (3) orally administrated PDE4 inhibitor at 1 mg/kg in contrast to the 0.3 mg/kg used in our study.

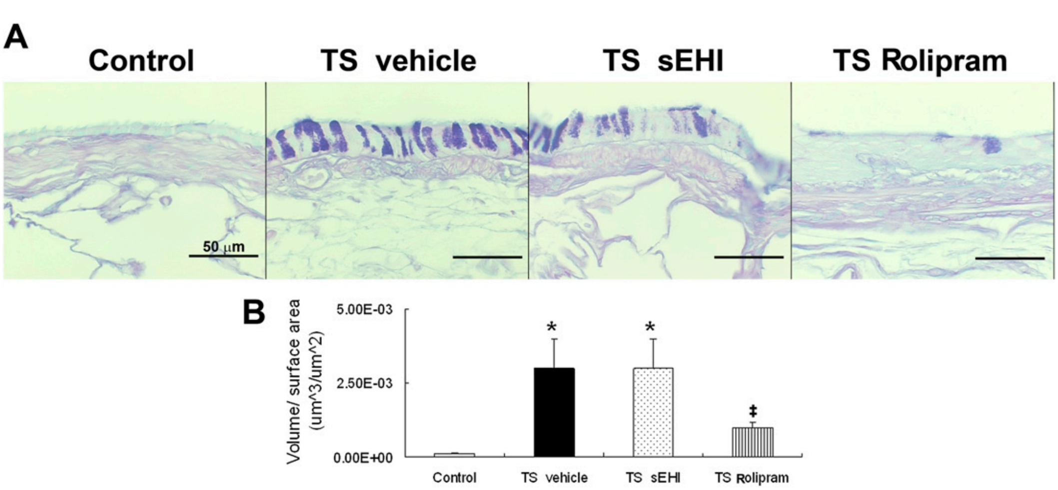

Figure 7. Effects of t-TUCB and Rolipram on TS exposure–induced mucin production. (*A*) Sections of the bronchial wall from filtered air (Control), TS-exposed SH rats with vehicle treatment (TS vehicle), sEHI treatment (TS sEHI), or Rolipram treatment (TS Rolipram) stained with alcian blue/periodic acid–Schiff for the detection of mucous glycoconjugate. (*B*) Blinded quantification of intraepithelial mucosubstances. *$P < 0.05$, TS-exposed groups were significantly different from the control group. ‡$P < 0.05$, treatment group with Rolipram was significantly different from the TS vehicle group.

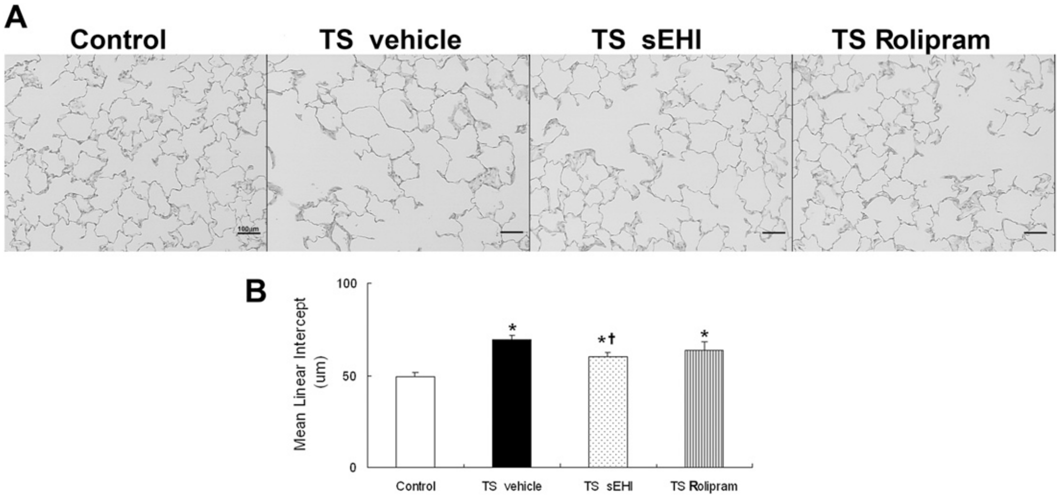

Figure 8. Effects of t-TUCB and Rolipram on TS exposure–induced airspace enlargement. (*A*) Sections of the parenchyma from filtered air (Control), TS-exposed SH rats with vehicle treatment (TS vehicle), sEHI treatment (TS sEHI), or Rolipram treatment (TS Rolipram) were stained with hematoxylin and eosin. (*B*) Blinded quantification of mean linear intercept. *$P < 0.05$, TS-exposed groups were significantly different from the control group. †$P < 0.05$, treatment group with sEHI t-TUCB was significantly different from the TS vehicle group.

Spond and colleagues (27) demonstrated a Rolipram dose–dependent decrease in the number of recoverable inflammatory cells from BALF.

Results from the present study suggest that the inhibitory activity of sEHI t-TUCB in airway obstruction is not temporally linked to proinflammatory cytokine production or the increase of total leukocytes in the BALF. Although the exact mechanisms underlying the bronchodilatory action of sEH inhibition are not clear, EETs were shown to modulate airway smooth muscle tone (29, 30). However, we failed to observe a significant correlation between EETs and airway resistance. In the present study, as expected, sEHI stabilized largely anti-inflammatory lipid epoxides, and reduced the production of largely proinflammatory lipid-1,2 diols. Schmelzer and colleagues (31) reported that EETs (the epoxides) transcriptionally down-regulated other inflammatory aspects of the arachidonic acid cascade (especially induced COX-2). In our experiment, the major metabolite of the COX-2 pathway, PGE2, was induced by smoke exposure and dramatically reduced by sEHI treatment. sEHI also reduced 13-HODE, which is the 12/15-lipoxygenase (12/15-LOX) metabolite of linoleic acid. A positive correlation was found between 13-HODE and airway resistance (R and Rn), as shown in Table 1. 13-HODE was implicated to play an important role in the induction of airway hyperresponsiveness *in vivo* (32). Thus, the attenuation of airway resistance by sEHI t-TUCB may occur by inhibiting the production of 13-HODE.

Both sEHI and PDE4 inhibitor dramatically decreased another very potent inflammatory mediator, 5-oxo-ETE, which is a downstream metabolite of the 5-LOX pathway, another inflammatory branch of the arachidonic acid pathway that produces inflammatory leukotrienes. 5-oxo-ETE was proven to act as a very potent chemoattractant for eosinophils and neutrophils, and elicits a variety of responses in these cells, including actin polymerization, calcium mobilization, integrin expression, and degranulation (33). In comparison, the PDE4 inhibitor Rolipram decreased the inflammatory mediators PGE2 and 5-oxo-ETE in a comparable manner. However, it failed to reduce 13-HODE. This may explain why a decrease in resistance in the Rolipram-treated group was not seen. Further studies are needed to clarify the precise molecular mechanisms and mode of action of sEHIs on airway obstruction. These data could provide the basis for a strong foundation for the development of COPD therapeutics.

The present study unequivocally demonstrates that TS exposure causes airspace enlargement, as shown by an increase in MLI in the SH rat. However, we did not observe a concordance in compliance. The reason for this disparity is not known, but the distribution of emphysema throughout the lung may not have been sufficiently widespread enough to affect airway compliance. Both sEHI t-TUCB and the PDE4 inhibitor Rolipram modestly blocked the emphysematous changes induced by TS exposure. We are not surprised that PDE4 inhibitors reduced TS-induced airspace enlargement. Prophylactic treatment with the PDE4 inhibitor Roflumilast was reported to prevent the development of emphysema in a chronic TS study performed in mice (26). In contrast, we only saw a trend of possible protection with Rolipram in this study. These differences may be attributable to dose, species sensitivity, or exposure conditions. A range of dosing regimens is therefore warranted to determine whether sEHIs inhibit emphysematous change in a dose-dependent manner.

Goblet-cell hyperplasia and metaplasia are well-established hallmarks of the airways of cigarette smokers, with and without COPD (34). In the present study, mucus hypersecretion was consistently observed in both proximal and distal airways in TS-exposed animals receiving vehicle treatment. However, treatment with sEHI did not ameliorate or exacerbate mucus accumulation at the dose used in this study, compared with the TS/vehicle group. On the other hand, treatment with the PDE4 inhibit resulted in significantly decreased intraepithelial airway mucin. Only limited information is available on the regulation of TS-induced mucus secretion. Several studies indicated that an increase in specific airway mucin genes, such as MUC5AC, are regulated by TS through the epidermal growth factor receptor (EFGR) signaling pathway (35, 36), or are related to c-Jun N-terminal protein kinase 1 signaling (37). Rolipram may affect mucin production through the EGFR regulation of MUC5AC expression, because Roflumilast was suggested to attenuate EGF-induced MUC5AC mRNA and protein expression in isolated human airway epithelial cells (38). We did not see a significant decrease of mucus production with sEHI treatment, which may be attributable to the dose: either the dose was not high enough to produce antimucus effects, or it does not affect mucin expression. This would indicate that a sEHI might need to be accompanied by mucolytic compounds in the clinical setting.

A number of studies demonstrated weight loss in animals exposed to TS (25, 39). Weight loss occurs in approximately 50% of patients with severe COPD, but it can also be seen in approximately 10–15% of patients with mild to moderate COPD (40). Weight loss is also a characteristic of advanced COPD (41). In patients with COPD, weight loss is mostly attributed to skeletal muscle atrophy and muscle dysfunction caused by a negative energy balance associated with a hypermetabolic state because of stress, pulmonary inflammation, and prolonged tissue hypoxia (42, 43). Consistent weight loss with TS exposure was observed in rats in the present study. Treatment with sEHI t-TUCB modestly, but significantly, reduced the degree of weight loss. Alterations in weight change by sEH inhibition cannot result from anti-inflammatory effects alone, because Rolipram did not significantly change weight reduction. Therefore, other mechanisms must be responsible.

Although the therapeutic potential for sEHIs to treat COPD appears promising, the potential for adverse or side effects must also be considered. sEHIs may exacerbate hypoxic pulmonary vasoconstriction and hypoxia-induced pulmonary vascular remodeling (44, 45), associated with increased EET generation and epoxygenase inhibition, thus increasing hypoxic pulmonary vasoconstriction (44). We are not aware whether the animals treated with sEHI in the present study developed pulmonary hypertension, because physiological measurements of this parameter were not performed. However, we did observe a significant decrease in VEGF concentration in the lungs with sEHI treatment, although no changes in pulmonary artery wall thickness with sEHI treatment were evident (data not shown). Further evaluation of the effect of sEHIs on the pulmonary vascular system is warranted.

In conclusion, we have characterized a TS-induced rat model of experimental COPD, confirming previous observations of airway inflammation, mucus hypersecretion, and enlargement of alveolar air space size. We also demonstrated an increase in airway resistance associated with airflow obstruction, similar to that found in human COPD. Treatment with a sEHI increased fatty acid epoxides and indirectly reduced the production of Th1 cytokines and proinflammatory lipid mediators, while minimizing airway obstruction and reducing weight loss in this rat model of COPD. These findings suggest sEHIs may play an important pharmacological role in the treatment of COPD.

Author disclosures are available with the text of this article at www.atsjournals.org.

Acknowledgments: The authors thank Janice Peake, Imelda Espiritu, Vish Seshachellam, and Dipti Munshi for technical assistance, and Dr. Suzette Smiley-Jewell for editorial assistance in the preparation of the manuscript.

References

1. Celli BR, Cote CG, Marin JM, Casanova C, Montes de Oca M, Mendez RA, Pinto Plata V, Cabral HJ. The body-mass index, airflow obstruction, dyspnea, and exercise capacity index in chronic obstructive pulmonary disease. *N Engl J Med* 2004;350:1005–1012.
2. Fox JC, Fitzgerald MF. The role of animal models in the pharmacological evaluation of emerging anti-inflammatory agents for the treatment of COPD. *Curr Opin Pharmacol* 2009;9:231–242.
3. Kubo S, Kobayashi M, Iwata M, Takahashi K, Miyata K, Shimizu Y. Disease-modifying effect of ASP3258, a novel phosphodiesterase Type 4 inhibitor, on subchronic cigarette smoke exposure–induced lung injury in guinea pigs. *Eur J Pharmacol* 2011;659:79–84.
4. Pauwels RA, Buist AS, Ma P, Jenkins CR, Hurd SS. Global strategy for the diagnosis, management, and prevention of chronic obstructive pulmonary disease: National Heart, Lung, and Blood Institute and World Health Organization Global Initiative for Chronic Obstructive Lung Disease (GOLD): executive summary. *Respir Care* 2001;46:798–825.
5. Barnes PJ, Shapiro SD, Pauwels RA. Chronic obstructive pulmonary disease: molecular and cellular mechanisms. *Eur Respir J* 2003;22:672–688.
6. Saetta M, Turato G, Maestrelli P, Mapp CE, Fabbri LM. Cellular and structural bases of chronic obstructive pulmonary disease. *Am J Respir Crit Care Med* 2001;163:1304–1309.
7. Hele DJ, Belvisi MG. Novel therapies for the treatment of inflammatory airway disease. *Expert Opin Investig Drugs* 2003;12:5–18.
8. Barnes NC, Qiu YS, Pavord ID, Parker D, Davis PA, Zhu J, Johnson M, Thomson NC, Jeffery PK. Antiinflammatory effects of salmeterol/fluticasone propionate in chronic obstructive lung disease. *Am J Respir Crit Care Med* 2006;173:736–743.
9. Cosio BG, Tsaprouni L, Ito K, Jazrawi E, Adcock IM, Barnes PJ. Theophylline restores histone deacetylase activity and steroid responses in COPD macrophages. *J Exp Med* 2004;200:689–695.
10. Fabbri LM, Beghe B, Yasothan U, Kirkpatrick P. Roflumilast. *Nat Rev Drug Discov* 2010;9:761–762.
11. Rennard SI, Schachter N, Strek M, Rickard K, Amit O. Cilomilast for COPD: results of a 6-month, placebo-controlled study of a potent, selective inhibitor of phosphodiesterase 4. *Chest* 2006;129:56–66.
12. Calverley PM, Sanchez-Toril F, McIvor A, Teichmann P, Bredenbroeker D, Fabbri LM. Effect of 1-year treatment with roflumilast in severe chronic obstructive pulmonary disease. *Am J Respir Crit Care Med* 2007;176:154–161.
13. Node K, Huo Y, Ruan X, Yang B, Spiecker M, Ley K, Zeldin DC, Liao JK. Anti-inflammatory properties of cytochrome P450 epoxygenase-derived eicosanoids. *Science* 1999;285:1276–1279.
14. Spector AA, Norris AW. Action of epoxyeicosatrienoic acids on cellular function. *Am J Physiol Cell Physiol* 2007;292:C996–C1012.
15. Inceoglu B, Schmelzer KR, Morisseau C, Jinks SL, Hammock BD. Soluble epoxide hydrolase inhibition reveals novel biological functions of epoxyeicosatrienoic acids (EETs). *Prostaglandins Other Lipid Mediat* 2007;82:42–49.
16. Jung O, Brandes RP, Kim IH, Schweda F, Schmidt R, Hammock BD, Busse R, Fleming I. Soluble epoxide hydrolase is a main effector of angiotensin II–induced hypertension. *Hypertension* 2005;45:759–765.
17. Xu D, Li N, He Y, Timofeyev V, Lu L, Tsai HJ, Kim IH, Tuteja D, Mateo RK, Singapuri A, *et al*. Prevention and reversal of cardiac hypertrophy by soluble epoxide hydrolase inhibitors. *Proc Natl Acad Sci USA* 2006;103:18733–18738.
18. Schmelzer KR, Inceoglu B, Kubala L, Kim IH, Jinks SL, Eiserich JP, Hammock BD. Enhancement of antinociception by coadministration of nonsteroidal anti-inflammatory drugs and soluble epoxide hydrolase inhibitors. *Proc Natl Acad Sci USA* 2006;103:13646–13651.
19. Smith KR, Pinkerton KE, Watanabe T, Pedersen TL, Ma SJ, Hammock BD. Attenuation of tobacco smoke–induced lung inflammation by treatment with a soluble epoxide hydrolase inhibitor. *Proc Natl Acad Sci USA* 2005;102:2186–2191.
20. Teague SV, Pinkerton KE, Goldsmith M, Gebremichael A, Chang S, Jenkins RA, Moneyhun JH. Sidestream cigarette smoke generation and exposure system for environmental tobacco smoke studies. *Inhal Toxicol* 1994;6:79–93.
21. Smith KR, Uyeminami DL, Kodavanti UP, Crapo JD, Chang LY, Pinkerton KE. Inhibition of tobacco smoke–induced lung inflammation by a catalytic antioxidant. *Free Radic Biol Med* 2002;33:1106–1114.
22. Yang J, Schmelzer K, Georgi K, Hammock BD. Quantitative profiling method for oxylipin metabolome by liquid chromatography electrospray ionization tandem mass spectrometry. *Anal Chem* 2009;81:8085–8093.
23. Bolton SJ, Pinnion K, Oreffo V, Foster M, Pinkerton KE. Characterisation of the proximal airway squamous metaplasia induced by chronic tobacco smoke exposure in spontaneously hypertensive rats. *Respir Res* 2009;10:118.
24. Zhong CY, Zhou YM, Pinkerton KE. NF-kappaB inhibition is involved in tobacco smoke–induced apoptosis in the lungs of rats. *Toxicol Appl Pharmacol* 2008;230:150–158.
25. Zheng H, Liu Y, Huang T, Fang Z, Li G, He S. Development and characterization of a rat model of chronic obstructive pulmonary disease (COPD) induced by sidestream cigarette smoke. *Toxicol Lett* 2009;189:225–234.
26. Hogg JC, Chu F, Utokaparch S, Woods R, Elliott WM, Buzatu L, Cherniack RM, Rogers RM, Sciurba FC, Coxson HO, *et al*. The nature of small-airway obstruction in chronic obstructive pulmonary disease. *N Engl J Med* 2004;350:2645–2653.
27. Spond J, Chapman R, Fine J, Jones H, Kreutner W, Kung TT, Minnicozzi M. Comparison of PDE 4 inhibitors, Rolipram and SB 207499 (Ariflo), in a rat model of pulmonary neutrophilia. *Pulm Pharmacol Ther* 2001;14:157–164.
28. Inceoglu B, Jinks SL, Schmelzer KR, Waite T, Kim IH, Hammock BD. Inhibition of soluble epoxide hydrolase reduces LPS-induced thermal hyperalgesia and mechanical allodynia in a rat model of inflammatory pain. *Life Sci* 2006;79:2311–2319.

29. Benoit C, Renaudon B, Salvail D, Rousseau E. EETs relax airway smooth muscle via an EpDHF effect: BK(Ca) channel activation and hyperpolarization. *Am J Physiol Lung Cell Mol Physiol* 2001;280:L965–L973.
30. Morin C, Sirois M, Echave V, Gomes MM, Rousseau E. EET displays anti-inflammatory effects in TNF-alpha stimulated human bronchi: putative role of CPI-17. *Am J Respir Cell Mol Biol* 2008; 38:192–201.
31. Schmelzer KR, Inceoglu B, Kubala L, Kim IH, Jinks SL, Eiserich JP, Hammock BD. Enhancement of antinociception by coadministration of nonsteroidal anti-inflammatory drugs and soluble epoxide hydrolase inhibitors. *Proc Natl Acad Sci USA* 2006;103:13646–13651.
32. Henricks PA, Engels F, van der Linde HJ, Garssen J, Nijkamp FP. 13-Hydroxy–linoleic acid induces airway hyperresponsiveness to histamine and methacholine in guinea pigs *in vivo*. *J Allergy Clin Immunol* 1995;96:36–43.
33. Powell WS, Rokach J. Biochemistry, biology and chemistry of the 5-lipoxygenase product 5-oxo-ETE. *Prog Lipid Res* 2005;44:154–183.
34. O'Donnell RA, Richter A, Ward J, *et al*. Expression of ErbB receptors and mucins in the airways of long term current smokers. *Thorax* 2004; 59:1032–1040.
35. Burgel PR, Nadel JA. Roles of epidermal growth factor receptor activation in epithelial cell repair and mucin production in airway epithelium. *Thorax* 2004;59:992–996.
36. Gensch E, Gallup M, Sucher A, Li D, Gebremichael A, Lemjabbar H, Mengistab A, Dasari V, Hotchkiss J, Harkema J, *et al*. Tobacco smoke control of mucin production in lung cells requires oxygen radicals AP-1 and JNK. *J Biol Chem* 2004;279:39085–39093.
37. Choi WI, Syrkina O, Kwon KY, Quinn DA, Hales CA. JNK activation is responsible for mucus overproduction in smoke inhalation injury. *Respir Res* 2010;11:172–179.
38. Mata M, Sarriá B, Buenestado A, Cortijo J, Cerdá M, Morcillo EJ. Phosphodiesterase 4 inhibition decreases MUC5AC expression induced by epidermal growth factor in human airway epithelial cells. *Thorax* 2005;60:144–152.
39. Guerassimov A, Hoshino Y, Takubo Y, Turcotte A, Yamamoto M, Ghezzo H, Triantafillopoulos A, Whittaker K, Hoidal JR, Cosio MG. The development of emphysema in cigarette smoke–exposed mice is strain dependent. *Am J Respir Crit Care Med* 2004;170:974–980.
40. Cukić V, Maglajlić J. Body weight loss in patients with chronic obstructive pulmonary disease. *Med Arh* 2007;61:175–181.
41. Schols AM, Soeters PB, Dingemans AM, Mostert R, Frantzen PJ, Wouters EF. Prevalence and characteristics of nutritional depletion in patients with stable COPD eligible for pulmonary rehabilitation. *Am Rev Respir Dis* 1993;147:1151–1156.
42. Agusti AG, Noguera A, Sauleda J, Sala E, Pons J, Busquets X. Systemic effects of chronic obstructive pulmonary disease. *Eur Respir J* 2003; 21:347–360.
43. American Thoracic Society, European Respiratory Society. Skeletal muscle dysfunction in chronic obstructive pulmonary disease: a statement of the American Thoracic Society and European Respiratory Society. *Am J Respir Crit Care Med* 1999;159(Suppl.):S1–S40.
44. Keseru B, Barbosa-Sicard E, Popp R, Fisslthaler B, Dietrich A, Gudermann T, Hammock BD, Falck JR, Weissmann N, Busse R. Epoxyeicosatrienoic acids and the soluble epoxide hydrolase are determinants of pulmonary artery pressure and the acute hypoxic pulmonary vasoconstrictor response. *FASEB J* 2008;22:4306–4315.
45. Pokreisz P, Fleming I, Kiss L, Barbosa-Sicard E, Fisslthaler B, Falck JR, Hammock BD, Kim IH, Szelid Z, Vermeersch P. Cytochrome P450 epoxygenase gene function in hypoxic pulmonary vasoconstriction and pulmonary vascular remodeling. *Hypertension* 2006;47:762–770.

Online Data Supplement

Use of a Soluble Epoxide Hydrolase Inhibitor in Smoke-induced Chronic Obstructive Pulmonary Disease

Lei Wang, Jun Yang, Lei Guo, Uyeminami Dale, Hua Dong, Bruce D. Hammock, Kent E. Pinkerton

Method:

2.1. Animals

Twelve-week-old male spontaneously hypertensive (SH) rats were purchased from Charles River Laboratories (Portage, MI). After arrival, all animals were housed in polycarbonate cages under a light cycle maintained at a 12-hour light-dark pattern with continuous access to food and water before, during, and after exposures. Animals were acclimated for one week before initialization of TS exposure. Animals were weighed weekly before and after tobacco smoke exposure. All animals were handled according to the Guide for the Care and Use of Laboratory Animals as adopted and promulgated by the US National Institutes of Health, and all procedures were performed under the supervision of the University Animal Care and Use Committee, IACUC approved protocol number 07-12922 (University of California, Davis).

2.2. Tobacco smoke exposure

Groups of four to eight SH rats were exposed to filtered air or to tobacco smoke, at a concentration of approximately 80–90 mg/ m3 total suspended particulates (TSP) for 4 weeks. Whole body exposure to cigarette smoke was performed (6 h/day, 3 days/week) using a TE10 smoke exposure system [E1] that combusts 3R4F research cigarettes (Tobacco and Health Research Institute, University of Kentucky, KY) with a 35 ml puff volume of 2 seconds duration, once each minute (Federal Trade Commission smoking standard).

2.3. Drugs and Delivery

The soluble epoxide hydrolase inhibitor (t-TUCB):*trans*-4-{4-[3-(4-**t**rifluoromethoxy-phenyl)-ureido]-**c**yclohexyloxy}-benzoic acid and phosphodiesterase type 4 inhibitor Rolipram: (*R/S*)-4-(3-cyclopentyloxy-4-methoxy-phenyl)pyrrolidin-2-one were delivered in drinking water one week prior to smoke exposure and continued throughout the 4-week study. The dose used for t-TUCB was 1.5 mg/kg and 0.3mg/kg for rolipram dissolved in PEG 400 and added to drinking water to give a final PEG concentration of 2% (v/v). Age-matched non-smoke-exposed and vehicle-administered animals were used as normal group animals.

2.4. Pulmonary Function Measurements

Eighteen hours post 4 weeks of TS exposure, rats were deeply anesthetized with Ketamine and Xylazine. A midline incision was made over the cervical trachea. Once the rats were tracheo-cannulated, the cannula was then connected to the Scireq Flexivent (Montreal, Canada) positive pressure ventilator, pulmonary mechanics measurement and data acquisition system. Animals were paralyzed by succinylcholine. The lung volume and pressure were measured twice while a standard respiratory cycle was simulated—once with the catheter open to room air, and once with it closed. The regular ventilation was delivered at a frequency of 90 breaths/min with a tidal volume of 10 ml/kg. Lung mechanics was evaluated using a forced oscillation technique. Measures of respiratory system input impedance was obtained that allows for the unique distinction between central and peripheral lung mechanics. A "snapshot perturbation" maneuver was imposed to measure resistance (R), compliance (C), and elastance (E) of the whole respiratory system (airways, lung, and chest wall). Forced oscillation perturbation was consequently applied, and resulted in Rn (central airway resistance), tissue damping (resistance) (G) and tissue elastance (H).

2.5. Tissue preparation

SH rats were anesthetized with an overdose of sodium pentobarbital following the pulmonary function test. The trachea was cannulated, the left lung bronchus tied, and the right lung lavaged with Ca^{2+}/Mg^{2+}-free Hank's buffered salt solution (HBSS) bronchoalveolar lavage (BAL) fluid (BALF) was collected in tubes and kept on ice prior to further processing. The lavaged lobes from the right lung were frozen in liquid nitrogen and stored at -80°C until use. For histology, the suture on the left lung bronchus was released, and the lung was inflated with 4% paraformaldehyde at 30 cm water pressure for 1 h, which was then followed by an immersion fixation, paraffin embedding and histopathology examination. Five-μm-thick paraffin-embedded tissue sections were deparaffinized and stained with hematoxylin and eosin (H&E) (American Master Tech Scientific, Lodi, CA), and periodic acid–Schiff staining (AB/PAS).

2.6. Bronchoalveolar Lavage (BAL) analysis

The BALF was centrifuged at 250g for 10 min at 4°C and the cell pellet was resuspended in Ca^{2+}/Mg^{2+}-free HBSS [E2]. Total cell number was determined using a hemocytometer. Cytospin slides (Shandon, Pittsburgh, PA) were prepared using aliquots of cell suspension that were then stained with Hema 3 (Fisher Scientific, Pittsburgh, PA). Cell differentials in BALF were assessed by counting mononuclear cells, neutrophils and eosinophils on cytocentrifuge slides using light microscopy (300 cells counted per sample).

2.7. Cytokine Analysis of lung homogenates

Lung homogenates from rats were analyzed for 24 different cytokines and chemokines (IL-1α, IL-1β, IL-2, IL-4, IL-5, IL-6, IL-7, IL-10, IL-12p70, IL-13, IL-17, IL-18, Eotaxin, G-CSF, GM-CSF, GROKC, IFN-γ, M-CSF, MIP-1α, MIP-3α, RANTES, TNF-α, vascular endothelial growth factor (VEGF), EPO) utilizing a fluorescent bead multiplex assay from Bio-Rad Laboratories (Hercules,CA). The assay was performed according to the manufacturer's instructions. The assay allows for the detection and quantitation of multiple cytokines at the protein level in a single sample using a 96-well microplate format. The standard curve for each cytokine was produced with a sensitivity of less than 10 pg/ml for each cytokine or chemokine.

2.8. Oxylipin measurements by liquid chromatography/mass spectrometry–mass spectrometry

Oxylipins from lung tissues were extracted by solid phase extraction (SPE) on 60 mg Waters Oasis-HLB cartridges (Milford, MA) according to the previously described method [E3]. Then the elutions from SPE cartridges were evaporated using a

Speedvac® system and reconstituted with 50 uL 200 nM 1-cyclohexyl ureido, 3-dodecanoic acid (CUDA) methanol solution. CUDA was used as an internal standard. The liquid chromatography system used for analysis was an Agilent 1200 SL liquid chromatograph series (Agilent Corporation, Palo Alto, CA). The autosamplar was kept at 4 °C. Liquid chromatography was performed on an Eclipse Plus C18 2.1 × 150 mm, 1.8 μm column (Agilent Corporation, Palo Alto, CA). Mobile phase A was water with 0.1% glacial acetic acid. Mobile phase B consisted of acetonitrile/methanol (84:16) with 0.1% glacial acetic acid. Gradient elution was performed at a flow rate of 250 μL/min. Chromatography was optimized to separate all analytes in 21.5 min. Analytes were eluted according to their polarity with the most polar analytes, prostaglandins and leukotrienes eluting first, followed by the hydroxy and epoxy fatty acids. The column was connected to a 4000 QTrap tandem mass spectrometer (Applied Biosystems Instrument Corporation, Foster City, CA) equipped with an electrospray source (Turbo V). The instrument was operated in negative multiple reaction monitor (MRM) mode. The optimized conditions and the MRM transitions were reported previously [E3]. Quality control samples were analyzed at a minimum frequency of 10 hours to ensure stability of the analytical calibration throughout the analysis. Analyst software 1.5 was used to quantify the results according to the standard curves.

2.9. Histopathology of the lung

Histology was performed using cross-sectional lung tissue slices containing the first and second intrapulmonary airway generations from rats. Five micron thick sections were cut from paraffin-embedded tissue blocks on a microtome. Sections were placed on glass slides and baked overnight at 37°C. Sections were subsequently deparaffinized and stained with the following: 1) hematoxylin and eosin (H&E) (American Master Tech Scientific, Lodi, CA) for measurement of airspace size of alveolar tissue, and 2) alcian blue/periodic acid-Schiff (AB/PAS) (American Master Tech Scientific, Lodi, CA) for mucous glycoconjugate detection. For each staining assay, a minimum of 6 fields were sampled from the central airway with an Olympus BH-2 microscope in a uniform random manner. To assess the fraction of the epithelial AB/PAS staining and mean linear intercept (MLI), images were projected onto a monitor and overlaid with a test grid generated by stereology toolbox software (Morphometrix, Davis, CA). Volume fraction was calculated as the number of total points hitting the objectives and total points falling within the reference space. Volume fraction = Pm (points of AB/PAS positive staining)/Pe(points of airway epithelium). MLI was calculated from the number of alveolar tissue intersections encountered in sampling templates. MLI = 2 (total number of sampled fields) (total number of test lines on the sampling template) (length of the test line, corrected for magnification) / (total number of intercepts).

2.10. Statistical Analysis: Data were analyzed and graphed using SAS version 8.2 statistical software (SAS Institute, Cary, NC). Data were expressed as mean ± SEM and generally analyzed using two-way ANOVA, and when significance was achieved, a Bonferroni post hoc test was used. For analysis of the correlation between oxylipins with airway obstructions based on FlexiVent measurements, linear regression will be used to analyze correlations by Pearson's correlation coefficient. The significance level considered will be $p<0.05$.

Reference:

E1. Teague, S.V., K.E. Pinkerton, M. Goldsmith, A Gebremichael, S. Chang, R.A.Jenkins and J.H. Moneyhun. , Sidestream cigarette smoke generation and exposure system for environmental tobacco smoke studies. Inhalation Toxicology, 1994(6): p. 79-93.

E2. Smith, K.R., et al., Inhibition of tobacco smoke-induced lung inflammation by a catalytic antioxidant. Free Radic Biol Med, 2002. 33(8): p. 1106-14.

E3. Yang, J., et al., Quantitative profiling method for oxylipin metabolome by liquid chromatography electrospray ionization tandem mass spectrometry. Anal Chem, 2009. 81(19): p. 8085-93.